Gault et al., http://www.jcb.org/cgi/content/full/jcb.201107137/DC1

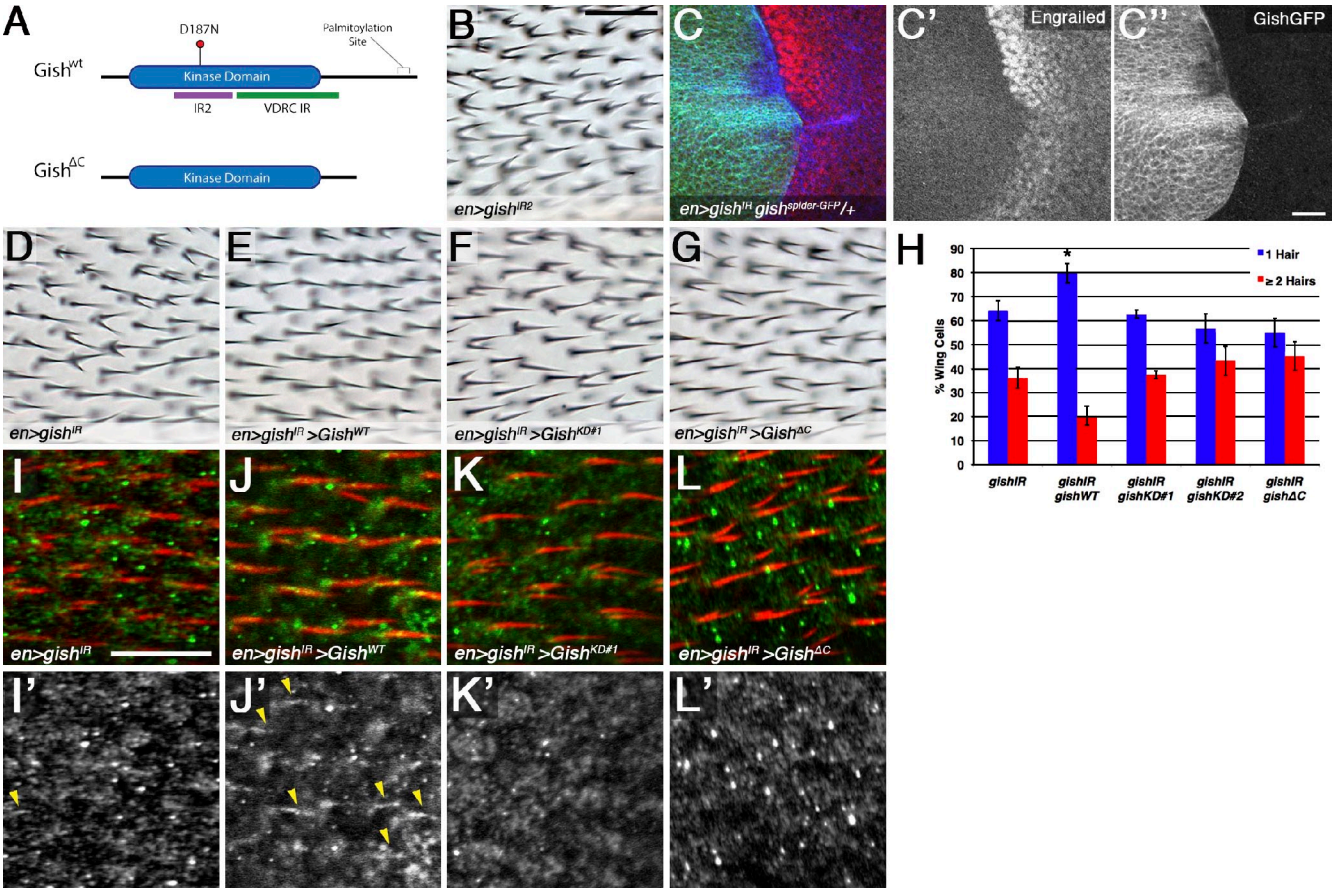

Figure S1. ***gish* requires kinase function and membrane localization for morphogenesis.** (A) Diagram representing RNAi target sequence location for two independent RNAi lines as well as the Gish^{WT} and Gish$^{\Delta C}$ structure. The *gish* kinase-dead (KD) D187N mutation is based on the comparable *Xenopus* CK1-γ mutant on a conserved residue in the ATPase domain (Davidson et al., 2005). (B) *en-Gal4* expression of a Vienna Drosophila RNAi Center–independent RNAi, *gish^{IR2}*, generates multiple trichomes similar to *gish^{IR}* and *FRT82-gish^{e01759}*. Distal is to the right. (C–C′′) *en-Gal4 UAS-gish^{IR}* eliminates *gish$^{spider\text{-}GFP}$*/+ (green) expression in the posterior *en* domain (red). (D and E) *UAS-myc-gish^{WT}* transgene coexpression partially rescues the *en-Gal4 UAS-gish^{IR}* phenotype. (F and G) Two independent *UAS-myc-gish^{KD}* transgenes (F and not depicted) and a ubiquitously localized *UAS-myc-gish$^{\Delta C}$* transgene (G) failed to rescue the phenotype. (H) Trichome quantification is graphically represented; the asterisk indicates a statistically significant rescue. Error bars show SDs (*, $P < 0.05$). (I–L) Rab11 localization is shown for the corresponding rescue experiments in D–G (yellow arrowheads indicate Rab11 association with the prehairs). Bars: (B and D–G) 25 µm; (C–C′′) 20 µm; (I–L) 10 µm.

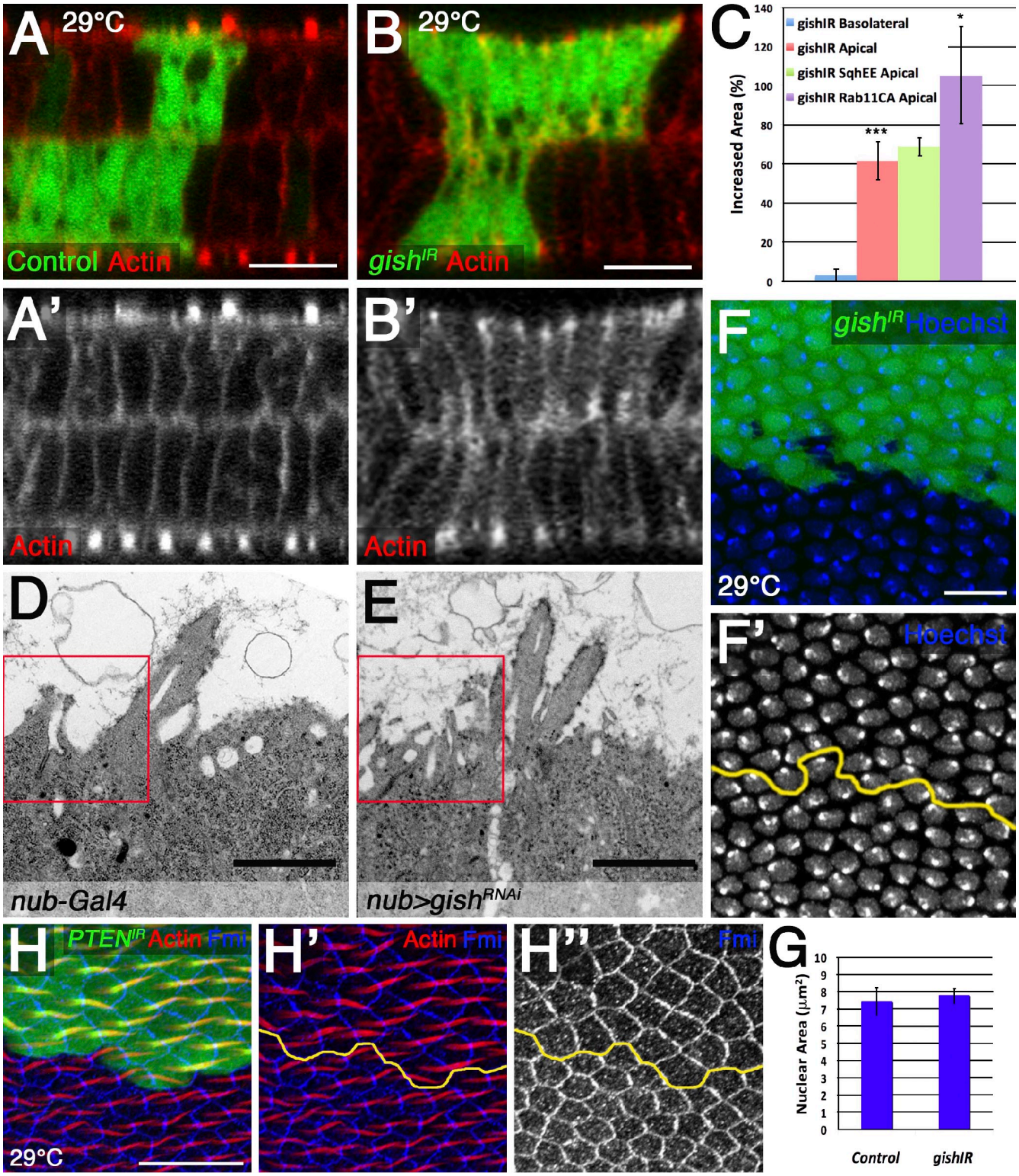

Figure S2. ***gish* regulates apical membrane growth.** (A–B′) Z sections of ∼28-h APF pupal (29°C) *actin-Gal4* FLP-out clones (GFP) during prehair formation stained with rhodamine-phalloidin (red). (A and A′) Control FLP-out clones (GFP). (B and B′) *UAS-gish*^{IR} expression induces apical membrane expansion. (C) The degree (percentage) of membrane expansion was measured within the xy plane (apical area was measured with Fmi protein, and basolateral was measured with cortical rhodamine-phalloidin staining below the nuclear level, graphically represented as the increase in cell area relative to adjacent control tissue; *, $P < 0.05$; ***, $P < 0.001$; unpaired *t* tests on pupal wings of three independent animals were scored). (D and E) TEM images display excess cellular projections in *nub-Gal4 UAS-gish*^{IR} tissue at 32–34 h APF (E) in comparison with *nub-Gal4* control tissue (D). Red boxes indicate comparable regions between the images. (F and F′) Confocal projections of whole nuclei staining (Hoechst, blue and monochrome in F and F′) of ∼28-h APF pupal wing (29°C) *actin-Gal4* FLP-out clones expressing *UAS-gish*^{IR} (GFP; clone border marked with yellow line) reveal no change in area. (G) Nuclear area was measured and graphically represented. (H–H′′) Approximately 28-h APF (29°C) *actin-Gal4* Flp-out clones (GFP; clone border marked with yellow lines) expressing *UAS-PTEN*^{IR} reveal no trichome defects associated with increase cell size (rhodamine-phalloidin, red; Fmi, blue in H and H′ and monochrome in H′′). Error bars show SDs. Bars: (A, B, and F) 10 µm; (D and E) 2 µm; (H) 20 µm.

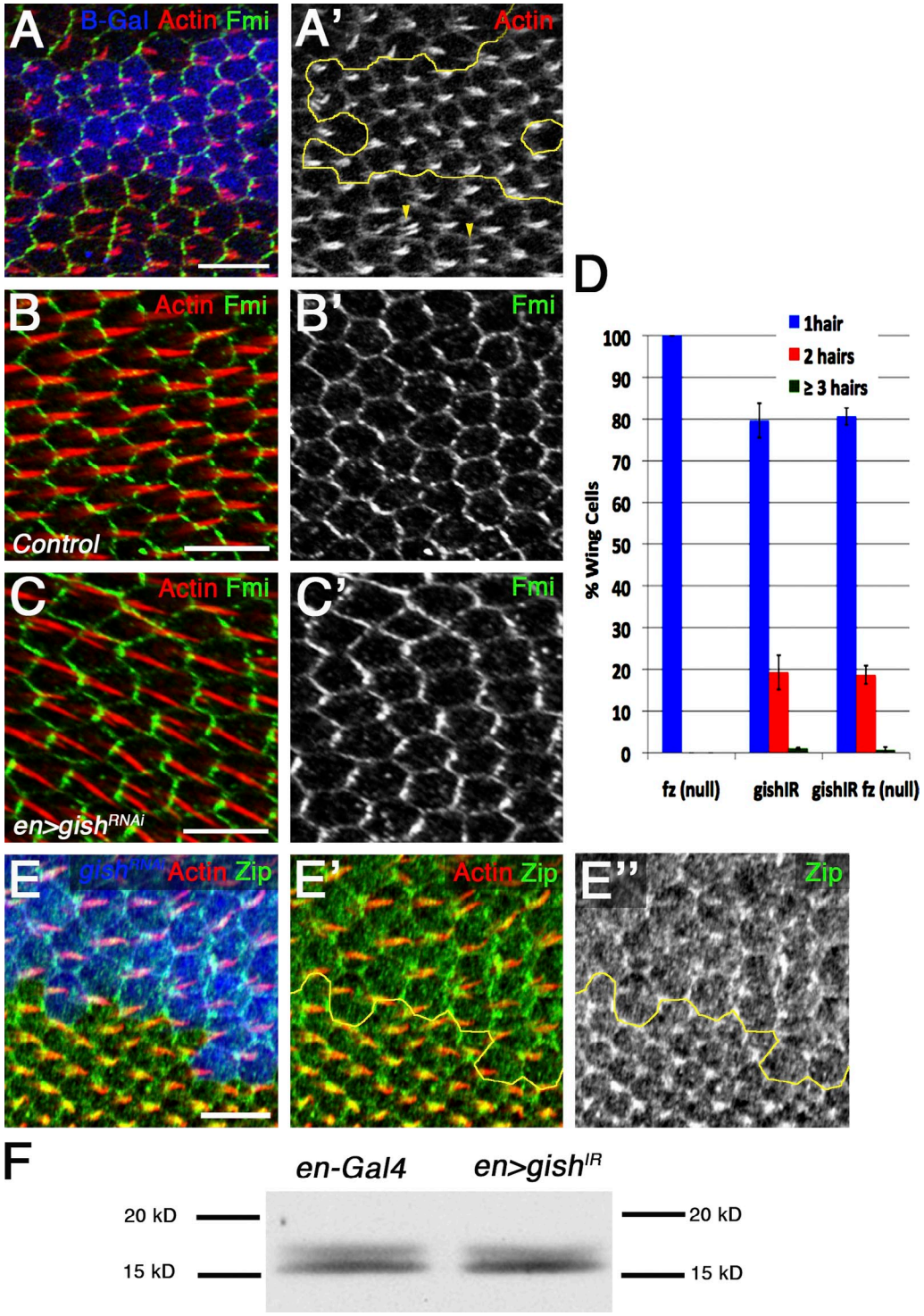

Figure S3. ***gish* function is independent of the Fz/Drok arm of the PCP pathway.** (A–A′′) FLP/FRT *gish*^{e01759} mutant clone (absence of β-galactosidase [B-Gal], blue; clone border marked with yellow line in A′) displaying multiple trichomes (red and monochrome in A and A′; yellow arrowheads) and asymmetric Fmi localization (green and monochrome in A). (B–C′) 32–34-h APF pupal wings displaying Fmi (green and monochrome) and rhodamine-phalloidin (red). *en-Gal4 UAS-gish*^{IR} expression does not affect asymmetric localization of Fmi (C and C′) compared with a control wing (B and B′). (D) The *nub-Gal4 UAS-gish*^{IR} trichome phenotype is not suppressed in an *fz*^{P21}/*fz*^{P21} (*fz* null) background (wings of three independent animals were scored). *Drok* (Rho-associated kinase) restricts trichome number downstream of PCP proteins Dsh and RhoA and functions to activate Zipper (Zip; the *Drosophila* myosin II homologue; Winter et al., 2001). We tested this Drok/Zip arm of PCP effector signaling by analyzing a dominant genetic interaction with the alleles *zip*^{1}, *Drok*^{2}, or a constitutively activated *spaghetti squash* (the *Drosophila* homologue of MRLC, *sqh*^{E20E21}; Winter et al., 2001) in the context of *gish*^{IR}. In any case, we failed to detect a significant modification of the *gish*^{IR} phenotype (not depicted). Error bars show SDs. (E–E′′) Zip staining (green in E and E′ and monochrome in E′′) demonstrates no change in levels or localization in *actin-Gal4* FLP-out *UAS-gish*^{IR} clones compared with adjacent tissue (blue; clone border marked with yellow lines). Note that Zip staining can be observed within developing prehairs in control and multiple trichome *gish*^{IR} tissue (rhodamine-phalloidin staining in red). (F) In third-instar wing discs expressing *UAS-gish*^{IR} via *en-Gal4* (29°C), no change in Sqh phosphorylation and thus Zip activation was observed in immunoblotting using a phosphospecific antibody for activated MRLC phosphorylated on a conserved serine (Ser21 in *Drosophila* corresponds to mammalian Ser19; Matsumura et al., 1998; Winter et al., 2001). Bars, 10 μm.

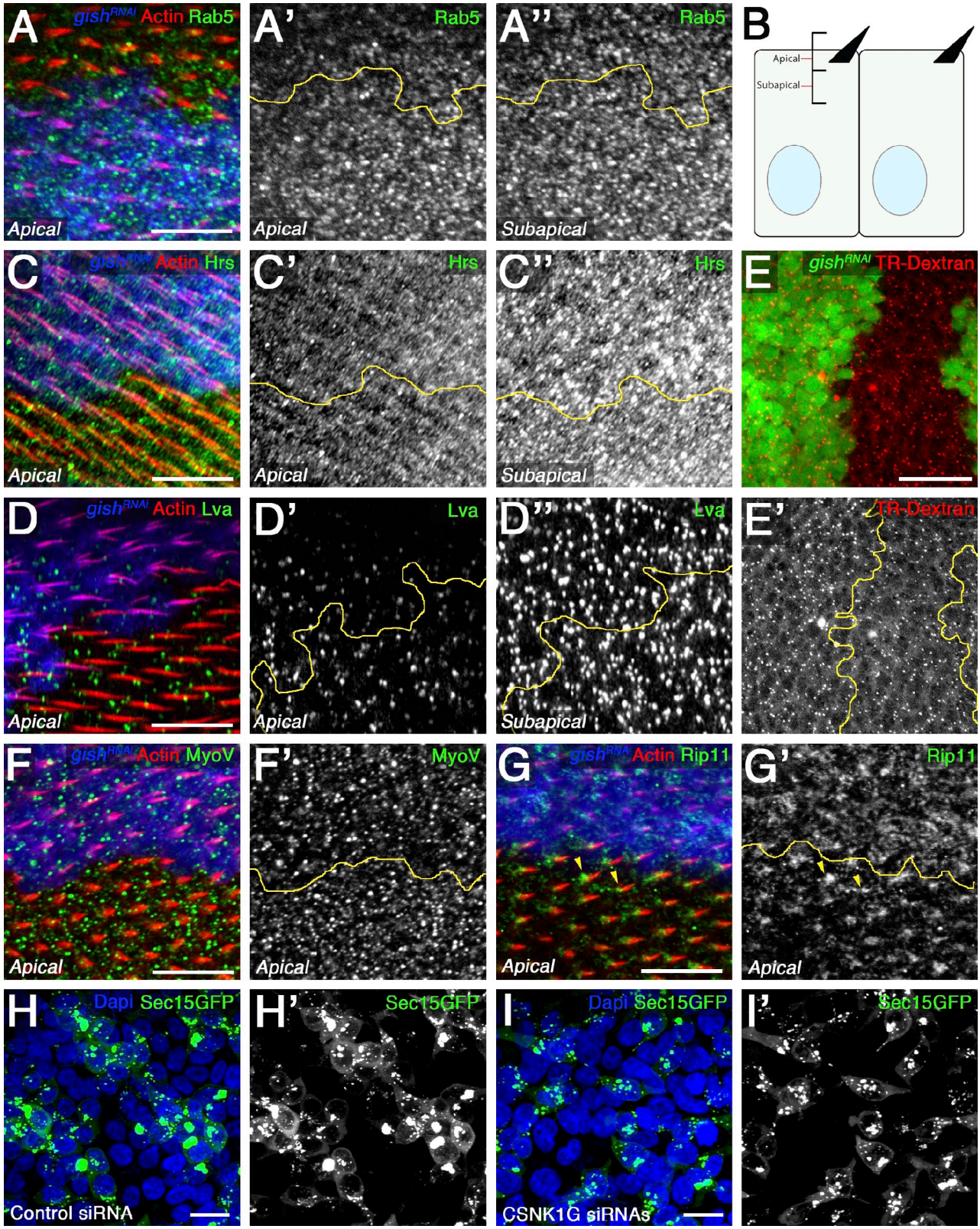

Figure S4. ***gish* function is specific to Rab11 trafficking.** (A–D′′) Examination of apical or subapical staining (see diagram in B) for Rab5 (green in A and monochrome in A′ and A′′), Hrs (green in C and monochrome in C′ and C′′), or Lava Lamp (Lva; green in D and monochrome in D′ and D′′) in *actin-Gal4 FLP-out UAS-gish*^{IR} clones (blue) revealed no difference in staining when compared with adjacent wild-type tissue. Distal is to the right. (B) Diagram defining the location of apical and subapical confocal projections in our assay (each bracket shows 1.2-µm projections). (E and E′) Dextran uptake (red and monochrome in E and E′) in third-instar wing disc *actin-Gal4 FLP-out UAS-gish*^{IR} clones (green). TR, Texas red. (F–G′) 32–32-h APF wings expressing *actin-Gal4 FLP-out UAS-gish*^{IR} clones (blue;) display normal MyoV and mislocalized dRip11 localization (green and monochrome in F and G and F′ and G′, respectively; yellow arrowheads indicate dRip11 enriched at the base of the prehair). (H and I) 293T cells transfected with Sec15GFP (gift from C. Mitchell) and control or siRNA targeting the three CSNK1G (mammalian CK1-γ) genes. Clone borders are marked with yellow lines. Bars: (A, C, D, F, and G) 10 µm; (E, H, and I) 20 µm.

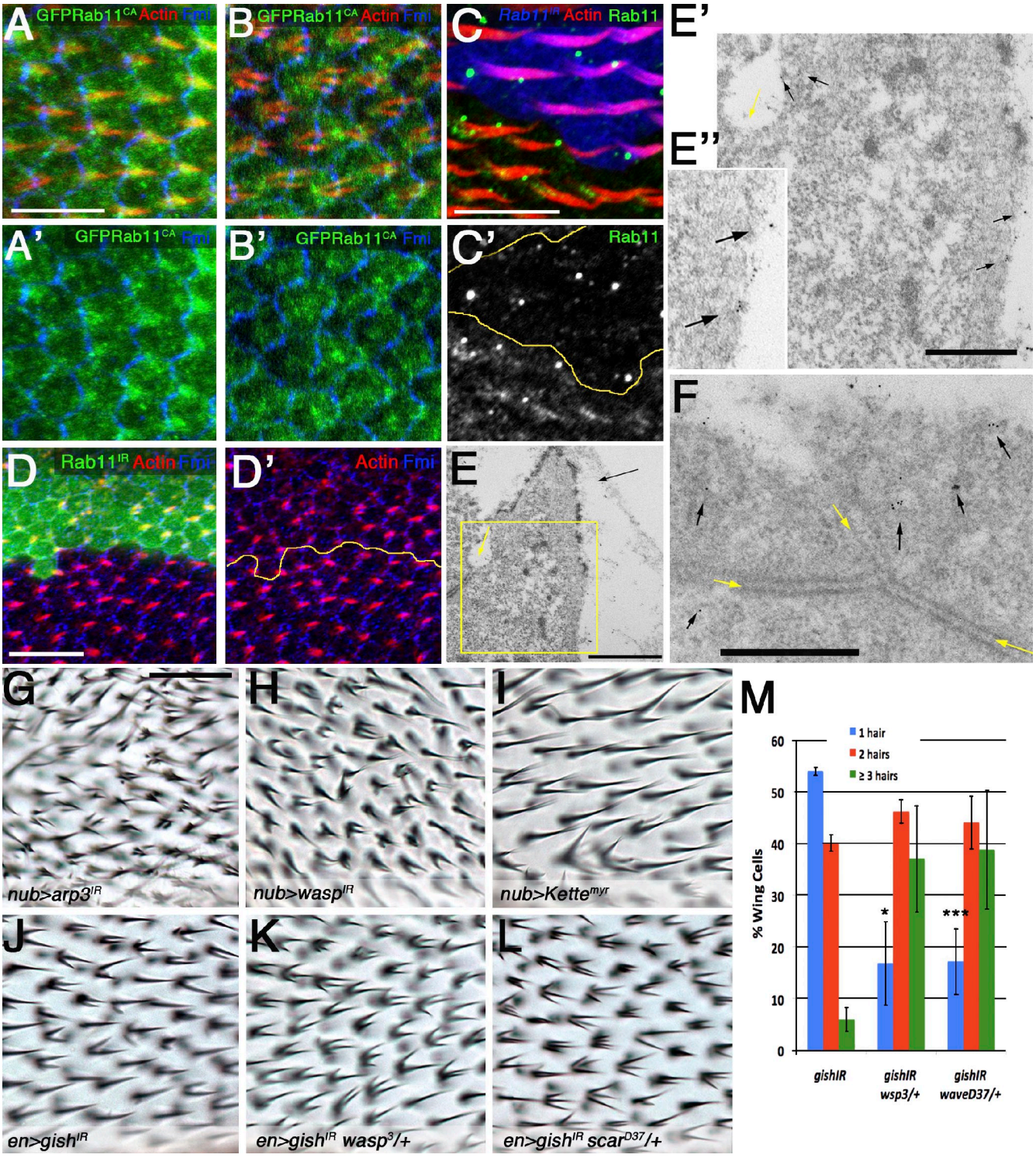

Figure S5. ***gish*, Rab11, and branched nucleators in trichome formation.** (A–B′) 32–34-h APF pupal wings expressing *nub-Gal4 UAS-YFP-Rab11*^{CA}. YFP-Rab11^{CA} was shown associated with the elongating trichome (red), whereas coexpression of *UAS-gish*^{IR} displayed a more diffuse YFP-Rab11^{CA} localization (B and B′). (C and C′) *Rab11*^{IR} *Flp-out* clones (blue and outlined in yellow) displayed reduced anti-Rab11 staining associated with the trichome, supporting that this localization pattern is specific to the endogenous Rab11 protein. (D and D′) *Rab11*^{IR} actin FLP-out clones displaying delayed and malformed trichomes (red). Cell membranes are labeled with Fmi (blue). (E′) Enlarged view present in the yellow area in E. Black arrows indicate 10-nm gold particles labeling GFP-Rab11. Note the association of GFP-Rab11 on the trichome membrane; distal is up, and apical is to the right. (F) Apical tangential section displaying Rab11 localization (black arrows; distal is up). Note the adherent junctions (yellow arrows in E, E′, and F). (G–I) nub-Gal4 expression of Arp3IR and WaspIR and overexpression of a myristoylated form of the Wasp regulator kette induce multiple trichomes (see also Fricke et al., 2009). (J–M) Removal of a single copy of wasp or scar/wave enhances the *gish*^{IR} phenotype (quantification in M). Unpaired *t* test was performed on three animals. Error bars show SDs (*, $P < 0.05$; ***, $P < 0.001$). Bars: (A–D) 10 µm; (E) 1 µm; (E′ and F) 0.5 µm; (G–L) 25 µm.

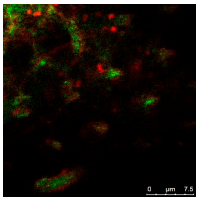

Video 1. **Rab11 vesicle dynamics during trichome initiation.** 36-h APF notum expressing YFP-Rab11^{WT} (green) in association with initiating prehair in the *pnr* domain (plasma membrane highlighted with mCD8-RFP, red). Images were acquired by time-lapse confocal microscopy using a confocal microscope (63×, 1.4 NA; SP5 DMI) and Leica software. Single confocal planes (1 µm) were taken at 6-s intervals for a total of 2 min.

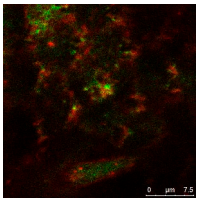

Video 2. **Rab11 vesicle dynamics are disrupted by *gish*^{IR} during trichome initiation.** 36-h APF notum expressing *gish*^{IR} and YFP-Rab11^{WT} (green) in the context of an initiating prehair in the *pnr* domain (plasma membrane highlighted with mCD8-RFP, red). Images were acquired by time-lapse confocal microscopy using a confocal microscope (63×, 1.4 NA; SP5 DMI) and Leica software. Single confocal planes (1 µm) were taken at 6-s intervals for a total of 2 min.

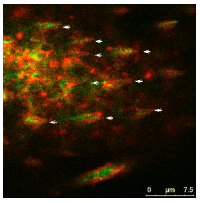

Video 3. **Rab11 vesicle dynamics during trichome elongation.** 38-h APF notum expressing YFP-Rab11^{WT} (green) in association with elongating prehairs in the *pnr* domain (white arrows; plasma membrane highlighted with mCD8-RFP, red). Images were acquired by time-lapse confocal microscopy using a confocal microscope (63×, 1.4 NA; SP5 DMI) and Leica software. Single confocal planes (1 µm) were taken at 6-s intervals for a total of 2 min.

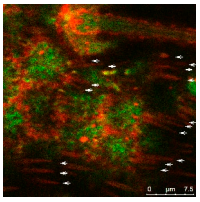

Video 4. **Rab11 vesicle dynamics are disrupted by *gish*^{IR} during trichome elongation.** 38-h APF notum expressing *gish*^{IR} and YFP-Rab11^{WT} (green) in the context of an elongating prehair in the *pnr* domain (white arrows; plasma membrane highlighted with mCD8-RFP, red). Images were acquired by time-lapse confocal microscopy using a confocal microscope (63×, 1.4 NA; SP5 DMI) with Leica software. Single confocal planes (1 µm) were taken at 6-s intervals for a total of 2 min.

References

Davidson, G., W. Wu, J. Shen, J. Bilic, U. Fenger, P. Stannek, A. Glinka, and C. Niehrs. 2005. Casein kinase 1 gamma couples Wnt receptor activation to cytoplasmic signal transduction. *Nature*. 438:867–872. http://dx.doi.org/10.1038/nature04170

Fricke, R., C. Gohl, E. Dharmalingam, A. Grevelhörster, B. Zahedi, N. Harden, M. Kessels, B. Qualmann, and S. Bogdan. 2009. *Drosophila* Cip4/Toca-1 integrates membrane trafficking and actin dynamics through WASP and SCAR/WAVE. *Curr. Biol.* 19:1429–1437. http://dx.doi.org/10.1016/j.cub.2009.07.058

Matsumura, F., S. Ono, Y. Yamakita, G. Totsukawa, and S. Yamashiro. 1998. Specific localization of serine 19 phosphorylated myosin II during cell locomotion and mitosis of cultured cells. *J. Cell Biol*. 140:119–129. http://dx.doi.org/10.1083/jcb.140.1.119

Winter, C.G., B. Wang, A. Ballew, A. Royou, R. Karess, J.D. Axelrod, and L. Luo. 2001. *Drosophila* Rho-associated kinase (Drok) links Frizzled-mediated planar cell polarity signaling to the actin cytoskeleton. *Cell*. 105:81–91. http://dx.doi.org/10.1016/S0092-8674(01)00298-7